JB
Journals.ASM.org

Cj1386, an Atypical Hemin-Binding Protein, Mediates Hemin Trafficking to KatA in *Campylobacter jejuni*

Annika Flint, Alain Stintzi

Ottawa Institute of Systems Biology, Department of Biochemistry, Microbiology and Immunology, Faculty of Medicine, University of Ottawa, Ottawa, ON, Canada

Catalase enzymes detoxify H_2O_2 by the dismutation of H_2O_2 into O_2 and H_2O through the use of hemin cofactors. While the structure and biochemical properties of catalase enzymes have been well characterized over many decades of research, it remained unclear how catalases acquire hemin. We have previously reported that Cj1386 is essential for ensuring proper hemin content in *Campylobacter jejuni* catalase (KatA) (A. Flint, Y. Q. Sun, and A. Stintzi, J Bacteriol 194:334–345, 2012). In this report, an in-depth molecular characterization of Cj1386 was performed to elucidate the mechanistic details of this association. Coimmunoprecipitation assays revealed that KatA-Cj1386 transiently interact *in vivo*, and UV-visible spectroscopy demonstrated that purified Cj1386 protein binds hemin. Furthermore, hemin titration experiments determined that hemin binds to Cj1386 in a 1:1 ratio with hexacoordinate hemin binding. Mutagenesis of potential hemin-coordinating residues in Cj1386 showed that tyrosine 57 was essential for hemin coordination when Cj1386 was overexpressed in *Escherichia coli*. The importance of tyrosine 57 in hemin trafficking *in vivo* was confirmed by introducing the *cj1386*^{Y57A} allele into a *C. jejuni* Δ*cj1386* mutant background. The *cj1386*^{Y57A} mutation resulted in increased sensitivity toward H_2O_2 relative to the wild type, suggesting that KatA was not functional in this strain. In support of this finding, KatA immunoprecipitated from the Δ*cj1386*+*cj1386*^{Y57A} mutant had significantly reduced hemin content compared to that of the *cj1386*^{WT} background. Overall, these findings indicate that Cj1386 is involved in directly trafficking hemin to KatA and that tyrosine 57 plays a key role in this function.

Hydrogen peroxide is a reactive oxygen species (ROS) that damages biological molecules such as DNA, protein, and lipids. H_2O_2 is inadvertently produced during cellular processes, such as aerobic metabolism, due to oxidation of respiratory dehydrogenases by molecular oxygen (1). Furthermore, Fenton chemistry results in the production of hydroxyl radicals from the reaction of H_2O_2 with ferrous ions (2). Therefore, detoxification of H_2O_2 by antioxidant enzymes is highly important in preventing cellular damage and/or death in living organisms.

Catalase is one of the major H_2O_2 detoxification enzymes present within cells, and it is found in almost all aerobically respiring organisms (3). Catalase functions by dismutating H_2O_2 into molecular oxygen and water (4). Although multiple crystal structures have been solved (5) and the biochemical properties of catalase have been extensively studied (4), the biogenesis of the enzyme has not yet been elucidated. The steps of catalase folding and hemin (defined as protoporphyrin IX containing a ferric ion) insertion, as well as potential chaperone proteins involved in this process, remain unknown. A recent report investigating genes important for catalase biogenesis was carried out in *Enterococcus faecalis* (6). By screening for catalase activity using a transposon mutant library, seven genes important for catalase activity were identified which code for the catalase itself (*katA*), RNA turnover global regulators (*rnjA* and *srmB*), NADH peroxidase (*npr*), stress response regulator (*etaR*), and membrane transport proteins (*oppBC*) (6). Excluding *katA*, the precise function of these genes for catalase activity requires further investigation; however, Baureder and Hederstedt speculate that these genes have an indirect role in catalase activity within the cell (6). Furthermore, despite in-depth characterization of heme transport into the cytoplasmic space of bacteria, very little is known about the potential proteins involved in trafficking heme to heme proteins within the cytoplasmic space.

Recently, our laboratory has identified a novel protein, Cj1386, that plays an important role in catalase biogenesis and the hemin content of *C. jejuni* KatA (7). We demonstrated that Cj1386 is required for optimal H_2O_2 detoxification within the cell and the presence of hemin within KatA. Specifically, KatA immunoprecipitated from a Δ*cj1386* mutant had a significant reduction in the hemin content associated with its KatA relative to KatA isolated from the wild-type strain. In turn, the decreased hemin content of KatA in the Δ*cj1386* mutant resulted in reduced catalase activity within the cell and, consequently, sensitivity to H_2O_2 (7).

In this report, we further characterize Cj1386 function to demonstrate its direct role in hemin trafficking within *C. jejuni*. Specifically, we investigated the biochemical and spectroscopic properties of the Cj1386 protein and also identified interacting proteins. We found that Cj1386 binds hemin at a 1:1 hemin-to-Cj1386 ratio and that tyrosine 57 is required for hemin coordination to Cj1386. Furthermore, coimmunoprecipitation experiments revealed that the KatA and Cj1386 proteins transiently interact. Overall, our results contribute to a greater fundamental understanding of hemin trafficking and catalase biogenesis within *C. jejuni* and establish that Cj1386 binds and trafficks hemin to KatA.

Received 24 September 2014 **Accepted** 19 December 2014

Accepted manuscript posted online 29 December 2014

Citation Flint A, Stintzi A. 2015. Cj1386, an atypical hemin-binding protein, mediates hemin trafficking to KatA in *Campylobacter jejuni*. J Bacteriol 197:1002–1011. doi:10.1128/JB.02346-14.

Editor: V. J. DiRita

Address correspondence to Alain Stintzi, astintzi@uottawa.ca.

Supplemental material for this article may be found at http://dx.doi.org/10.1128/JB.02346-14.

Copyright © 2015, American Society for Microbiology. All Rights Reserved.

doi:10.1128/JB.02346-14

TABLE 1 Bacterial strains used in this study

Strain or plasmid	Genotype or description[a]	Source or reference
E. coli strains		
DH5α	*endA1 hsdR17* (r_K^- m_K^-) *supE44 thi-1 recA1 gyrA relA1* Δ(*lacZYA-argF*)*U169 deoR*[ϕ80d*lac*Δ(*lacZ*ΔM15)]	Invitrogen
BL21(DE3)	F^- *ompT gal dcm lon hsdS*$_B$ (r_B^- m_B^-) λ(DE3)	Novagen
Rosetta	F^- *ompT hsdS*$_B$(r_B^- m_B^-) *gal dcm* pRARE Cam^r	Novagen
AS1082	BL21(DE3)(pGST+*katA*) Amp^r	Flint et al. (7)
AS1091	Rosetta(pGST+*cj1386*) Amp^r Cam^r	This study
AS1138	Rosetta(pGST+*cj1386*^{Y57A}) Amp^r Cam^r	This study
AS1142	Rosetta(pGST+*cj1386*^{H46A}) Amp^r Cam^r	This study
AS1150	Rosetta(pGST+*cj1386*^{C89A}) Amp^r Cam^r	This study
C. jejuni strains		
AS144	NCTC 11168	National Collection of Type Cultures
AS216	AS144 Δ*perR*::Cam^r	Palyada et al. (38)
AS433	AS144 Δ*katA*::Cam^r	Palyada et al. (38)
AS942	AS144 Δ*cj1386*::Cam^r	Flint et al. (7)
AS1028	AS942 *cj1386*::Cam^r Kan^r	Flint et al. (7)
AS1139	AS942 *cj1386*^{Y57A}	This study
AS1144	AS942 *cj1386*^{H46A}	This study
AS1149	AS942 *cj1386*^{C89A}	This study
Plasmids		
pRY111	Cam^r resistance gene	Yao et al. (39)
pRRK	Cloning vector used for complementation of mutants, Kan^r	Reid et al. (40)
pUC19	Cloning vector, Amp^r	New England Biolabs
pGST	Protein expression vector with GST tag and IPTG inducible promoter	Sheffield et al. (8)

[a] Cam^r, chloramphenicol resistance gene; Kan^r, kanamycin resistance gene; Amp^r, ampicillin resistance gene.

TABLE 2 Primers used in this study

Primer name	Primer sequence[a] (5′–3′)
Cj1386_NcoI	**GCCATGGCT**ATGACAACTCTTAGTTTAGA
Cj1386_NotI	**GCGGCCGC**TAAAAGGGGCGGTTCCTATC
Cat-SE	TGCTCGGCGGTGTTCCTTTCCAAG
Cat-AS	TGCGCCCTTTAGTTCCTAAAGGGT
AR56-AS	CATCCTCTTCGTCTTGGTAGC
ak233-SE	GCAAGAGTTTTGCTTATGTTAGCAG
ak234-SE	GAAATGGGCAGAGTGTATTCTCCG
ak235-SE	GTGCGGATAATGTTGTTTCTG
Y57A-SE	GCTTGCAGCTGCTAATAATTCT
Y57A-AS	ATAAGCAAGCTATCGCCTTTATGA
H46A-SE	TTTAAAAACTGCTAAAGGCGATAG
H46A-AS	TTTACATTTAAACCTGCTTCTATCATG
C89A-SE	AGCGGGAGTTGCTTTTAAAGGAT
C89A-AS	AATGGGGTTTGTCCACGATCGTTTT

[a] Restriction sites are in boldface.

MATERIALS AND METHODS

Bacterial strains, plasmids, and growth conditions. *Escherichia coli* DH5α, BL21, and Rosetta strains were grown at 37°C under aerobic conditions in Luria-Bertani (LB) broth or on LB agar plates supplemented with 100 μg/ml ampicillin, 50 μg/ml kanamycin, and/or 50 μg/ml chloramphenicol as required. *Campylobacter jejuni* NCTC 11168 was cultured under microaerophilic conditions (83% N_2, 4% H_2, 8% O_2, and 5% CO_2) at 37°C in a MACS-VA500 workstation (Don Whitley, West Yorkshire, England). *C. jejuni* strains were grown on Mueller-Hinton (MH) agar plates supplemented with 10 μg/ml kanamycin and/or 20 μg/ml chloramphenicol as required, in biphasic flasks, or in minimal essential medium alpha (MEMα; Invitrogen) supplemented with 20 mM sodium pyruvate. The bacterial strains and plasmids used in this study are listed in Table 1.

Purification of *C. jejuni* Cj1386 and anti-Cj1386 antiserum production. Overexpression of Cj1386 was performed in *E. coli* Rosetta cells using the protein expression vector pGST as described previously (8). Briefly, the *C. jejuni cj1386* gene was PCR amplified using Pfx high-fidelity polymerase (Invitrogen) and the cj1386_NcoI and cj1386_NotI primers listed in Table 2. The amplified gene was cloned into digested pGST vector using NcoI and NotI restriction sites, followed by transformation of the construct into *E. coli* DH5α cells. Sequencing was performed to confirm the absence of polymerase-introduced mutations in the *cj1386* gene. The pGST-*cj1386*^{WT} construct subsequently was transformed into *E. coli* Rosetta cells for Cj1386 overexpression. The *E. coli* Rosetta pGST-*cj1386*^{WT} strain was grown in 1 liter of LB broth supplemented with 100 μg/ml of ampicillin and 50 μg/ml chloramphenicol to an optical density at 600 nm (OD_{600}) of 0.6 at 37°C with continual shaking. Induction of protein expression was performed by addition of isopropyl-β-D-thiogalactopyranoside (IPTG; 500 μM) and overnight incubation with continual shaking at 18°C. The cells then were pelleted, resuspended in phosphate-buffered saline (PBS; 137 mM NaCl, 2.7 mM KCl, 10 mM Na_2HPO_4, 2 mM KH_2PO_4, pH 7.4) containing protease inhibitor (Roche), and lysed by sonication. Cell membranes and debris were removed by centrifugation at 16,060 × *g* for 15 min. The cell lysate containing the GST-Cj1386 fusion protein then was affinity purified using glutathione-Sepharose 4B resin according to the manufacturer's instructions (GE Healthcare). Cleavage of the glutathione *S*-transferase (GST) tag from Cj1386 was performed on the resin by addition of tobacco etch virus (TEV) protease (8) and gentle shaking overnight at 4°C. The Cj1386 protein was washed from the resin the following day using 6 washes of 500 μl of PBS buffer and concentrated using a 10-kDa-cutoff centrifugal filter unit (Millipore). Concentrated Cj1386 protein was further purified by size exclusion chromatography using the AKTA fast protein liquid chromatography (FPLC) system equipped with a Superdex-75 column (GE Healthcare) with PBS as the filtration buffer. Purified protein was frozen and stored at −20°C until use.

Cj1386 antibody production was performed by Immuno-Precise Antibodies Limited (Victoria, BC, Canada). For each rabbit, a preimmune bleed was performed prior to the primary immunization with the Cj1386 antigen (0.5 mg) using complete Freund's antigen. Over the course of the project, each rabbit received 4 additional boosts with Cj1386 antigen (0.25 mg) using incomplete Freund's antigen followed by a terminal bleed and serum collection. Anti-Cj1386 antiserum was stored at −20°C until use.

Preparation of apo-Cj1386. Hemin was extracted from purified Cj1386 using the acid-acetone method as described previously (9, 10). HCl-acetone solution was prepared by adding 0.34 volumes of 12 M HCl to 30 volumes of acetone. One milliliter of 50 μM purified Cj1386 was slowly added to 10 volumes of cold HCl-acetone, and the precipitated protein was pelleted by centrifugation at 16,060 × *g* for 15 min. The heme extraction step was repeated once more, and the precipitated Cj1386 protein was resuspended in 4 M urea. Buffer exchange with 100 mM NaCl, 20 mM Tris, pH 7.4, was performed using a 10-kDa-cutoff centrifugal filter unit (Millipore). UV-visible (UV-vis) spectra of 10 μM prepared apo-

Cj1386 protein (see below) was used to confirm successful hemin removal by the absence of a Soret peak. Apo-Cj1386 was stored at −20°C until use.

UV-vis spectroscopy and hemin titration. All spectroscopy measurements were recorded at room temperature using a sealed quartz cuvette with a 1-cm path length on a SpectraMax Plus 384 spectrophotometer (Molecular Devices). Hemin stock solutions (2.5 mM hemin in 20 mM NaOH) were prepared fresh, diluted to 500 μM in 100 mM NaCl, 20 mM Tris, pH 7.4, buffer, and added in 1 μM increments to 500 μl of 10 μM apo-Cj1386 or 500 μl of 100 mM NaCl, 20 mM Tris, pH 7.4, buffer. Spectral readings were taken 5 min after addition of hemin to the protein and reference solutions. Hemin-Cj1386 binding spectra from 260 nm to 700 nm were determined by subtracting the nonbound background hemin at each concentration titrated. The hemin stoichiometric binding ratio was determined by the absorbance value of the Soret peak at each concentration. Dissociation constants, K_d, were calculated with GraphPad Prism v.6 using nonlinear regression assuming one-site, specific ligand binding. Statistical differences between K_d values were calculated using a paired *t* test, with $P < 0.05$ considered significant.

Site-directed mutagenesis of Cj1386. The *cj1386*^{H46A}, *cj1386*^{Y57A}, and *cj1386*^{C89A} mutant alleles were constructed by PCR amplification of both pGST-Cj1386^{WT} and pRRK-Cj1386^{WT} using Phusion hot start II high-fidelity DNA polymerase with primers H46A-SE, H46A-AS, Y57A-SE, Y57A-AS, C89A-SE, and C89A-AS (cartridge filtered; Invitrogen). PCR products were purified with the PureLink PCR purification kit (Invitrogen) followed by 5′ phosphorylation of 25 ng of PCR product using T4 polynucleotide kinase (New England BioLabs) for 30 min at 37°C. Phosphorylated products were ligated using Quick T4 DNA ligase (New England BioLabs) for 5 min at room temperature and subsequently transformed into *E. coli* DH5α. Mutation of the *cj1386* gene in each of the pGST-*cj1386* and pRRK-*cj1386* constructs was confirmed by sequencing. The resulting pGST-*cj1386* and pRRK-*cj1386* H46A/Y57A/C89A mutant plasmids then were transformed into *E. coli* Rosetta and *C. jejuni* Δ*cj1386* mutant strains, respectively. Confirmation of the chromosomal insertion of the *C. jejuni* Δ*cj1386* mutant strain with the H46A/Y57A/C89A plasmids was performed by PCR using the AR56 and AK233-235 primers.

Sequence analysis. Homologs of Cj1386 were identified by protein BLAST analysis using the nonredundant protein sequence database and standard protein BLAST parameters (protein-protein BLAST algorithm) (11). Cj1386 homologs from different Gram-negative bacteria were selected and aligned using Clustal Omega (12) on EBI (13). The multiple-sequence alignments shown in Fig. 3 were constructed using Jalview (14) and Adobe Illustrator 3.

Disc inhibition assay. *C. jejuni* NCTC11168 wild-type, mutant, and complemented strains were grown on MH agar plates supplemented with chloramphenicol and/or kanamycin as required for 3 days under microaerophilic conditions at 37°C. Strains then were cultured in MH broth in biphasic flasks overnight. The overnight cultures were diluted in MH broth to an OD_{600} of 1, and 4 ml was added to 100 ml molten MH agar (cooled to 50°C). The agar subsequently was poured in equal volumes into petri dishes and allowed to solidify before the placement of 6-mm paper discs on the agar surface. Ten microliters of 3% H_2O_2 was added to each disc, and the plates were incubated for 28 h under microaerophilic conditions at 37°C, followed by measurement of the diameter of inhibition (mm). Each mutant and complemented strain was tested in at least biological triplicate. The averages of the clear zones were used to determine if statistical significance existed between the mutant, complemented, and wild-type strains using analysis of variance (ANOVA). $P < 0.05$ was considered statistically significant.

Coimmunoprecipitation of Cj1386 and KatA. Coimmunoprecipitation of Cj1386 or KatA from the Δ*perR* mutant strain was performed using protein A-conjugated Dynabeads (Invitrogen). Briefly, the *C. jejuni* Δ*perR* mutant strain was grown under microaerophilic conditions in MEMα to mid-log phase (OD_{600} of 0.2) at 37°C and cross-linked in 0.75% formaldehyde for 2 min. Tris-HCl, pH 8.0, subsequently was added to the cultures at a final concentration of 250 mM to quench remaining formaldehyde, and the cells were incubated for a further 10 min. Cultures were centrifuged at 6,000 × *g* for 10 min to pellet the cells, and the pellets were resuspended in radioimmunoprecipitation assay (RIPA) buffer (50 mM Tris-HCl, pH 7.4, 140 mM NaCl, 1 mM EDTA, 1% Triton X-100, 0.1% sodium deoxycholate, 0.1% SDS) containing a bacterial protease inhibitor cocktail (Sigma). Cells were lysed by sonication on ice, and cellular debris was removed by centrifugation at 16,060 × *g* for 5 min. Dynabeads were prepared by addition of 250 μg of anti-KatA or anti-Cj1386 sera, or 25 μg affinity-purified anti-Fur antibody (15) (diluted in 0.02% Tween-PBS), to 50 μl beads and rotated end over end for 1 h at room temperature. Antibodies were covalently conjugated to the beads using bis(sulfosuccinimidyl) suberate (BS^3; Invitrogen) according to the manufacturer's instructions. Two milligrams of cross-linked Δ*perR* mutant lysate was added to the beads and incubated for 1 h at room temperature with end-over-end rotation. Beads were washed 3 times with 200 μl RIPA buffer, transferred to a clean tube, resuspended in 20 μl 2× Laemmli buffer, and heated at 70°C for 10 min to dissociate the protein complexes from the antibody-conjugated beads. Immunoprecipitated protein was separated from the magnetic beads and transferred to a clean tube. Eluted protein samples were heated further at 99°C for 25 min to reverse formaldehyde cross-links. Protein samples were separated by SDS-PAGE on a 12% polyacrylamide gel. Immunoprecipitated proteins were visualized using Western blot analysis as described previously (7), using anti-Cj1386 (0.5 μg/ml) or anti-KatA (0.1 μg/ml) polyclonal antibodies. Use of a high-sensitivity chemiluminescent detection substrate (SuperSignal West Femto; Pierce) was utilized to visualize target proteins. Experiments were performed in at least biological triplicate.

Hemin quantification assays. Hemin content of KatA protein isolated from wild-type *C. jejuni* NCTC11168 and the Δ*cj1386*+*cj1386*^{Y57A} strain was quantified using the hemin assay kit (Biovision, Mountain View, CA) as described previously (7). KatA was immunoprecipitated from wild-type *C. jejuni* NCTC11168 and Δ*cj1386*+*cj1386*^{Y57A} strains according to the same method as that described above, with slight modifications to the cell lysis, bead preparation, and elution steps. Briefly, cells were harvested without formaldehyde cross-linking and resuspended in PBS containing a bacterial protease inhibitor cocktail (Sigma). Anti-KatA antibody was added to the Dynabeads without covalently linking the antibody to the beads. Elution of KatA protein was carried out by addition of 20 μl of 50 mM glycine, pH 2.8, to the Dynabeads. Samples were incubated at room temperature for 2 min with end-over-end rotation and subsequently transferred to a clean tube. The samples were brought to neutral pH by the addition of 1 M Tris, pH 7.4. Samples were visualized by SDS-PAGE run on a 10% denaturing gel followed by Coomassie blue staining. Total hemin concentration was assayed from 40 ng of KatA protein prepared from each immunoprecipitated sample, and the assay was performed according to the manufacturer's instructions (hemin assay kit; Biovision, Mountain View, CA). Experiments were performed in biological triplicate. Statistical significance was determined by the Student *t* test, with *P* values of <0.05 considered significant.

RESULTS

Cj1386 is a hemin-binding protein. To date, the structure, biochemical properties, and biological importance of catalase enzymes have been well studied in both prokaryotic and eukaryotic organisms. However, the order of events and potential chaperones involved in the biogenesis of catalase have not been clearly elucidated. Recently, our laboratory identified a key role for Cj1386 in promoting proper hemin content in catalase within *Campylobacter jejuni* (7). Therefore, to demonstrate and further investigate the molecular mechanism of Cj1386 in hemin trafficking and KatA biogenesis, we purified Cj1386 and assessed it for hemin binding by absorption spectroscopy.

Purification of Cj1386 yielded a solution with a yellowish hue, suggesting that Cj1386 is a hemin-binding protein (Fig. 1A). UV-

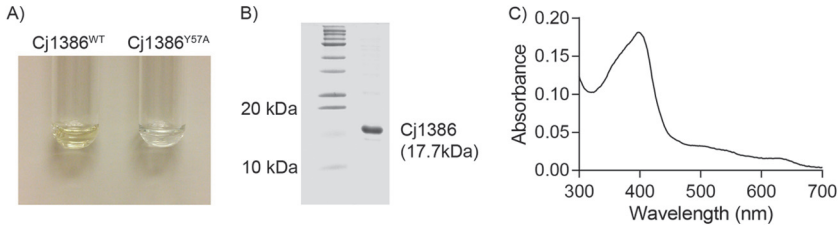

FIG 1 Cj1386 is a hemin-binding protein. (A) Purified Cj1386^{WT} and Cj1386^{Y57A} protein solutions at 50 μM. Cj1386^{WT} has a yellowish hue, in contrast to Cj1386^{Y57A}, which is colorless. (B) Cj1386 purification after size exclusion chromatography. Five microliters of purified protein was loaded and separated on a 14% denaturing SDS-PAGE gel. (C) Absorption spectrum of 10 μM purified Cj1386 in 100 mM NaCl, 20 mM Tris, pH 7.4, at 22°C.

vis spectroscopy further supported that Cj1386 binds hemin by the presence of a Soret peak, which is a characteristic of hemin-binding proteins (Fig. 1C) (16). Quantification of the hemin content from purified Cj1386 revealed that a significant proportion of the purified protein was bound to hemin (Fig. 1C). Therefore, to determine the hemin binding stoichiometry of Cj1386 and dissociation constant, hemin was removed from purified Cj1386 using an acid-acetone method to prepare apo-Cj1386 protein (see Materials and Methods). Complete hemin removal from Cj1386 was confirmed by the absence of a Soret peak when 10 μM apo-Cj1386 was analyzed by absorbance spectroscopy (Fig. 2A). Reconstitution of apo-Cj1386 with increasing concentrations of hemin showed one prominent Soret peak at 412 nm with shoulder bands at 550 nm and 640 nm (Fig. 2A). The iron atom of hemin is coordinately bound to four nitrogen atoms of the hemin pyrrole rings, allowing for either one (referred to as pentacoordinate binding) or two (hexacoordinate binding) additional bonds to be made on the proximal and/or distal side of the iron atom when ligating to proteins. The presence of a Soret band at 412 nm suggests low-spin, hexacoordinate hemin binding to Cj1386 (17, 18). Reduction of holo-Cj1386 with 1 mM dithiothreitol (DTT) shifted the Soret peak at 412 nm to 422 nm and the α/β bands from 550 nm and 640 nm to 554 nm and 630 nm, in accordance with the proposed hemin coordination (Fig. 2B). Titration of 10 μM apo-Cj1386 with hemin revealed a 1:1 molar binding ratio, demonstrating that one hemin molecule binds to one Cj1386 subunit (Fig. 2C). The hemin binding constant, K_d, for Cj1386 is $4.3 \times 10^{-6} \pm 0.3 \times 10^{-6}$ M for the 412-nm peak. The K_d value for Cj1386 indicates that it has a weaker affinity for hemin than other heme binding proteins, such as bovine serum albumin (BSA) and myoglobin (6.4×10^{-9} and 1.3×10^{-14} M, respectively) (Table 3). Furthermore, Cj1386 has a hemin affinity similar to that observed for the *Pseudomonas aeruginosa* heme trafficking protein PhuS (K_d of 0.2×10^{-6} M) (19). Overall, the hemin-binding af-

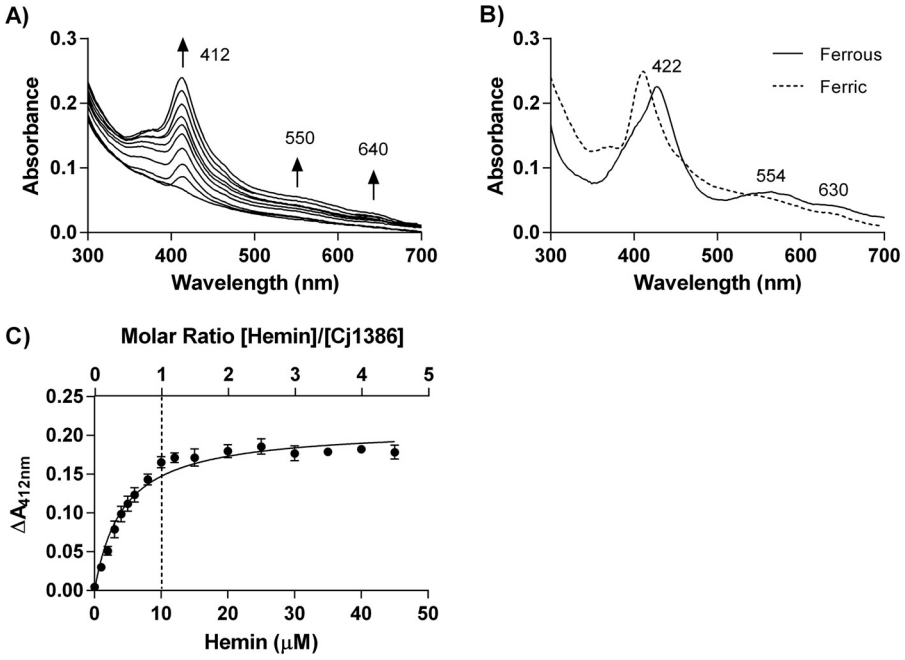

FIG 2 Cj1386 displays hexacoordinate hemin binding with 1:1 binding stoichiometry. (A) Absorption spectra of 10 μM apo-Cj1386 in the presence of increasing concentrations of hemin. Hemin was extracted from purified Cj1386 using acid acetone to produce apo-Cj1386. Hemin titration was performed in 1 μM increments against 10 μM apo-Cj1386 in 100 mM NaCl, 20 mM Tris, pH 7.4. Arrows represent the direction of increased absorbance readings upon hemin addition. (B) Absorption spectrum of 10 μM ferrous holo-Cj1386 after reduction of 10 μM ferric holo-Cj1386 using 1 mM sodium dithionite in 100 mM NaCl, 20 mM Tris, pH 7.4. (C) Hemin-Cj1386 binding stoichiometry determined by difference absorbance values at 412 nm. The dashed line represents the concentration of Cj1386 and hemin that yield a 1:1 hemin-to-Cj1386 binding ratio. Error bars represent the standard errors as determined from hemin titration from 2 independent protein purifications.

TABLE 3 Binding affinities of heme proteins

Heme protein and peak	K_d (M)	Source or reference
BSA	5×10^{-9}	41
PhuS	0.2×10^{-6}	19
Myoglobin	1.3×10^{-14}	42
Cj1386^{WT}, 412 nm	4.3×10^{-6}	This study
Cj1386^{Y57A}		
372 nm	7.7×10^{-6}	This study
412 nm	6.9×10^{-6}	This study

finities for Cj1386 support a role for this protein in hemin trafficking.

Tyrosine 57 is important for hemin affinity to Cj1386 and hemin trafficking in *C. jejuni*. Hemin titration of apo-Cj1386 determined that one hemin prosthetic group binds per Cj1386 subunit. Inspection of the Cj1386 protein sequence did not reveal any known hemin-binding motif, such as those characterized for cytochrome (20) and catalase enzymes (21). Therefore, to determine residues involved in hemin binding, the Cj1386 protein sequence was aligned against Cj1386 homologs from different bacterial species to identify conserved residues that potentially were important for hemin binding. Heme coordination with proteins commonly occurs through histidine, tyrosine, methionine, or cysteine residues (22). A multiple-sequence alignment of Cj1386 against homologs of *Campylobacter coli* CCO11496, *Helicobacter hepaticus* YahD, *Arcobacter butzleri* Abu0197, and *Pseudomonas putida* Pp1834 is shown in Fig. 3. From the sequence alignments, histidine 46, tyrosine 57, and cysteine 89 were found to be highly conserved and consequently were targeted for site-directed mutagenesis and assessed for hemin occupancy.

Overexpression and purification of the Cj1386^{Y57A} mutant did not yield a solution with a yellow hue, in contrast to purified Cj1386^{WT}, suggesting that hemin was no longer bound to the purified Cj1386^{Y57A} mutant (Fig. 1A). Indeed, absorption spectroscopy of 10 μM purified Cj1386^{WT} and 10 μM Cj1386^{Y57A} revealed that the Cj1386^{Y57A} mutant no longer purified with a fraction of the protein coordinated to hemin, as illustrated by the absence of a Soret peak (Fig. 4A). Although the Y57A mutant did not purify with hemin bound to the protein, the mutation did not prevent hemin coordination *in vitro*. The Cj1386^{Y57A} mutant displayed an absorption spectra different from that observed for reconstituted Cj1386^{WT} but still bound hemin at a 1:1 stoichiometry (Fig. 4B and 5). Reconstitution of apo-Cj1386^{Y57A} with increasing concentrations of hemin showed two prominent Soret peaks at 372 nm and 412 nm, with shoulder bands at 550 nm and 640 nm (Fig. 4B and 5A). The presence of the Soret band at 412 nm suggests low-spin, hexacoordinate hemin binding to Cj1386 (17, 18), whereas a peak at 372 nm indicates high-spin, pentacoordinate hemin binding. Interestingly, the presence of two Soret peaks suggests two configurations of hemin binding upon titration, with possible equilibrium between the pentacoordinate and hexacoordinate hemin-binding modes. The K_d value for the 412-nm peak displayed a significantly weaker affinity for hemin ($P = 0.0025$) at $6.9 \times 10^{-6} \pm 1.1 \times 10^{-6}$ M for Cj1386^{Y57A} compared to $4.3 \times 10^{-6} \pm 0.3 \times 10^{-6}$ M for Cj1386^{WT} (Table 3). The hemin affinity at the 372-nm peak for Cj1386^{Y57A} was $7.7 \times 10^{-6} \pm 1.0 \times 10^{-6}$ M (Table 3). Overall, these results suggests that the tyrosine 57 residue plays an important role in the affinity of hemin to Cj1386 when competing for hemin inside bacterial cells, as observed by the absence of a Soret peak from *E. coli*-purified Cj1386^{Y57A} protein. However, Cj1386^{Y57A} still is able to coordinate hemin when titrated with hemin in a noncompetitive assay, albeit with weaker hemin binding at the hexacoordinate 412-nm position.

To assess the biological significance of the Y57A mutant phe-

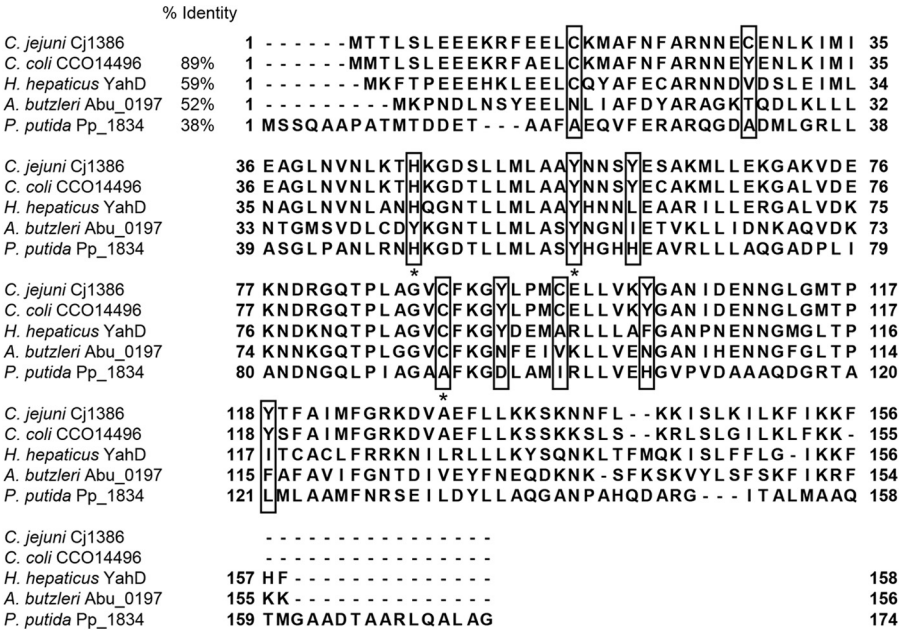

FIG 3 Multiple-sequence alignment of ankyrin-repeat Cj1386 homologs. Tyrosine, cysteine, and histidine residues present in the Cj1386 sequence are boxed. Asterisks represent highly conserved residues potentially involved in hemin coordination. Percent sequence identity for each protein sequence relative to that of Cj1386 is reported. Protein name and bacterial species are listed.

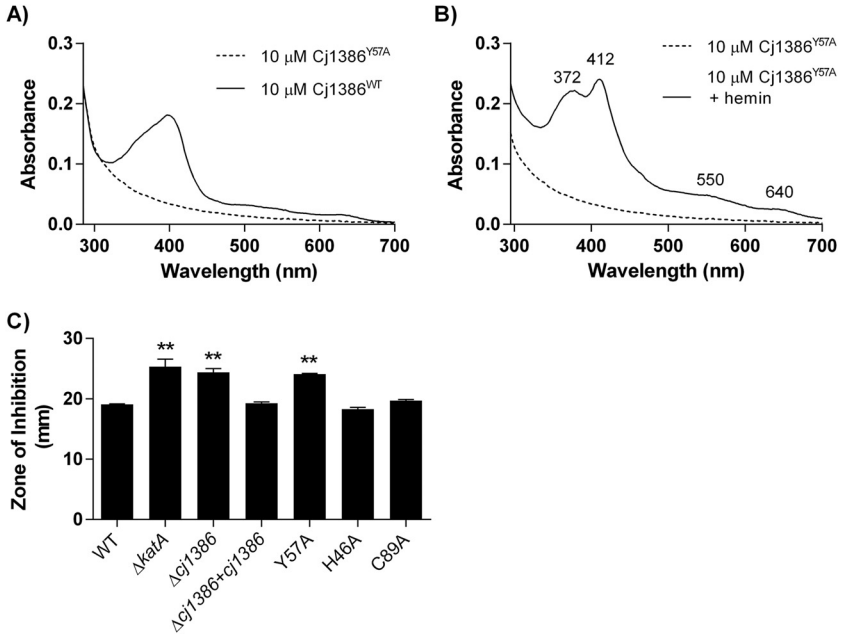

FIG 4 Tyrosine 57 is important for hemin affinity to Cj1386. (A) Absorption spectra of 10 μM Cj1386^{WT} and 10 μM Cj1386^{Y57A} in 100 mM NaCl, 20 mM Tris, pH 7.4. (B) Absorption spectra of 10 μM Cj1386^{Y57A} and 10 μM Cj1386^{Y57A} plus 10 μM hemin in 100 mM NaCl, 20 mM Tris, pH 7.4. (C) Growth inhibition analysis of wild-type *C. jejuni* and the Δ*katA*, Δ*cj1386*, Δ*cj1386*+*cj1386*^{WT}, and Δ*cj1386*+*cj1386*^{Y57A} mutants. Strains were exposed to 10 μl of H_2O_2 and incubated under microaerophilic conditions at 37°C for 28 h, followed by measurement of the diameter of growth inhibition. Experiments were repeated in biological triplicate. Statistical significance was determined by ANOVA, with $P < 0.05$ considered significant.

notype, a *C. jejuni* strain expressing a Cj1386^{Y57A} allele in a Δ*cj1386* mutant background was constructed and tested for hydrogen peroxide sensitivity using growth inhibition assays. As shown in Fig. 4C, the Δ*cj1386*+*cj1386*^{Y57A} mutant strain had an increased sensitivity toward H_2O_2 of 24.11 mm, whereas that for wild-type *C. jejuni* was 19.06 mm ($P < 0.001$). Furthermore, the increased sensitivity toward H_2O_2 of 24.11 mm in the Δ*cj1386*+*cj1386*^{Y57A} strain was not significantly different from the

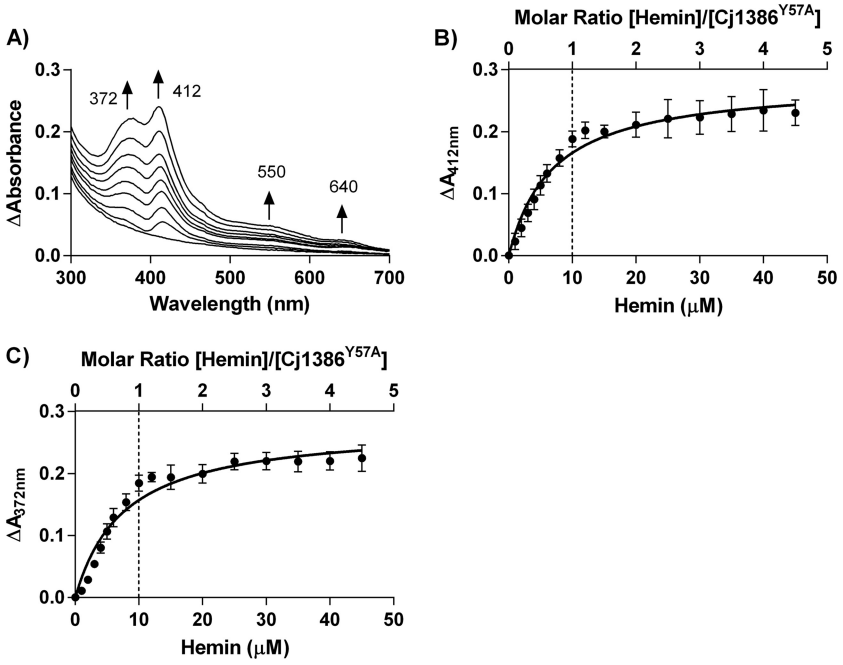

FIG 5 Y57A Cj1386 can be reconstituted with hemin and displays 1:1 hemin-binding stoichiometry. (A) Absorption spectra of Cj1386^{Y57A} when titrated with hemin at 1 μM increments against 10 μM apo-Cj1386^{Y57A} in 100 mM NaCl, 20 mM Tris, pH 7.4. Arrows represent the direction of increased absorbance readings upon hemin addition. (B and C) Differential absorption spectra of Cj1386^{Y57A} at Soret peaks at 372 nm and 412 nm. The dashed line represents the concentration of Cj1386^{Y57A} and hemin that yield a 1:1 heme-to-Cj1386^{Y57A} binding ratio. Error bars represent the standard errors as determined from hemin titration from 2 independent protein purifications.

TABLE 4 Hemin quantification of KatA immunoprecipitated from *C. jejuni* NCTC11168 and Δ*cj1386*+*cj1386*^{Y57A} strains[a]

Source of immunoprecipitated KatA	Concn of KatA subunits (nM)	Concn of hemin (nM)	Hemin/KatA ratio	Source or reference
C. jejuni NCTC11168	7.4	6.99 ± 0.19	0.94	7
Δ*cj1386* strain	7.4	0.19 ± 0.10*	0.03	7
Δ*cj1386*+*cj1386*^{WT} strain	7.4	6.41 ± 0.54	0.87	7
Δ*cj1386*+*cj1386*^{Y57A} strain	7.4	0.29 ± 0.18*	0.04	This study

[a] The amount of hemin is represented as the mean concentration of hemin detected ± standard errors (in nM) for equal starting concentrations of KatA protein for each strain tested. Experiments were repeated in biological triplicate. Student's *t* test was used to determine statistical significance, with *P* values of <0.05 (*) considered significant.

Δ*cj1386* mutant diameter of inhibition of 24.39 mm, demonstrating that the Y57 residue is required to restore the phenotype of the Δ*cj1386* mutant to wild-type sensitivity (Fig. 4C). Indeed, the sensitivity of the Δ*cj1386*+*cj1386*^{Y57A} strain also was similar to that of the Δ*katA* mutant strain (25.30 mm [7]; not significant at $P > 0.05$). This result highlights that loss of tyrosine 57 results in a severe inability of *C. jejuni* to resist H_2O_2 at levels comparable to those in the absence of the catalase enzyme itself. Importantly, sensitivity of the Δ*cj1386* mutant toward H_2O_2 was restored in the Δ*cj1386*+*cj1386*^{WT} strain. To verify that the Δ*cj1386*+*cj1386*^{Y57A} strain H_2O_2 phenotype is due to the change of amino acid at the tyrosine 57 residue and not due to the absence of protein expression, Western blot analysis was performed and confirmed the presence of Cj1386^{Y57A} expression in the Δ*cj1386*+*cj1386*^{Y57A} strain at levels comparable to that of the wild type (see Fig. S1 in the supplemental material).

The hypersensitivity of the *cj1386*^{Y57A} allele to H_2O_2 indicates that tyrosine 57 is key for Cj1386 function within *C. jejuni*. The absorption spectra of Cj1386^{Y57A} expressed and purified from *E. coli* cells revealed that Y57 plays an important role for hemin affinity to Cj1386; specifically, the Cj1386^{Y57A} protein was purified without coordinated hemin. Thus, it is probable that Cj1386^{Y57A} within the Δ*cj1386*+*cj1386*^{Y57A} mutant is either unable to bind or is outcompeted for hemin binding within *C. jejuni*. Consequently, the Cj1386^{Y57A} protein would not be able to traffic hemin to KatA, resulting in decreased H_2O_2 detoxification within the cell. Indeed, when KatA was immunoprecipitated from the Δ*cj1386*+*cj1386*^{Y57A} strain (see Fig. S2 in the supplemental material) and the hemin content was quantified, a significant reduction in the hemin-KatA ratio was observed (Table 4). KatA is a tetrameric protein consisting of four identical subunits, with each subunit coordinating one hemin prosthetic group. The hemin content of the Δ*cj1386*+*cj1386*^{Y57A} strain was found to have a hemin-KatA ratio of 0.04 per KatA subunit, compared to 0.94 for the wild-type strain. Furthermore, the hemin-KatA ratio for the Δ*cj1386*+*cj1386*^{Y57A} strain was similar to that previously obtained for the Δ*cj1386* mutant (0.03), highlighting the importance of Y57 for optimal function within *C. jejuni*.

Purification of the Cj1386^{H46A} and Cj1386^{C89A} proteins both yielded a yellow-hued solution, suggesting that hemin is bound to the Cj1386^{H46A} and Cj1386^{C89A} proteins. Absorbance spectroscopy of the Cj1386^{H46A} and Cj1386^{C89A} proteins confirmed this result, with both Cj1386^{H46A} and Cj1386^{C89A} proteins displaying a broad Soret peak (data not shown). Although histidine 46 and cysteine 89 appear to be highly conserved (Fig. 3), mutation of these residues did not affect the ability of the protein to coordinate hemin following purification. Furthermore, the Δ*cj1386*+*cj1386*^{H46A} and Δ*cj1386*+*cj1386*^{C89A} mutants were not affected in their sensitivity toward H_2O_2 relative to the wild type using disc inhibition assays (Fig. 4). Thus, in contrast to the Δ*cj1386*+*cj1386*^{Y57A} mutant, mutation of these amino acids did not significantly affect the function of Cj1386 in *C. jejuni*.

Cj1386 and KatA interact. To further assess the role of Cj1386 in hemin trafficking to KatA, coimmunoprecipitation experiments were performed to probe for a KatA-Cj1386 interaction. Initial experiments using non-cross-linked whole-cell lysates to pull down KatA or Cj1386, followed by Western blotting, did not identify any interaction between KatA and Cj1386. Given the role of Cj1386 in hemin trafficking to KatA, we hypothesized that any direct interaction between the two proteins is transient. Thus, it is probable that the absence of any detectable interaction between KatA and Cj1386 was due to the lack of formation of a stable protein complex. Consequently, coimmunoprecipitation of KatA and Cj1386 was performed after the cells were fixed by formaldehyde cross-linking to capture any transient interactions between the proteins. Furthermore, due to the low expression levels of Cj1386 in wild-type *C. jejuni* (see Fig. S3 in the supplemental material), we subsequently probed for a KatA-Cj1386 interaction in a Δ*perR* mutant background in which *cj1386* is derepressed (7). Detection of a KatA-Cj1386 protein-protein interaction was observed by coimmunoprecipitation of KatA from cross-linked proteins isolated from the Δ*perR* mutant strain and subsequent probing for Cj1386 using Western blot analysis (Fig. 6). As seen in Fig. 6, a band corresponding to Cj1386 was detected when KatA was pulled down from the Δ*perR* mutant lysate. Immunoprecipitation

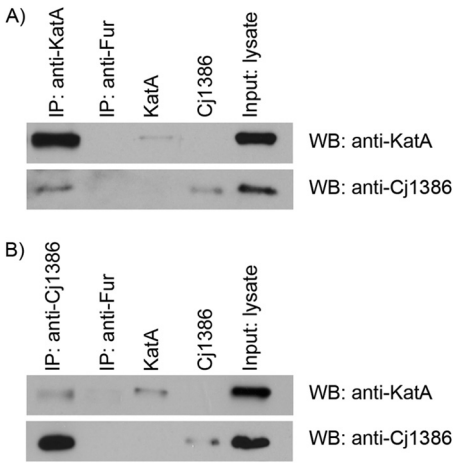

FIG 6 Cj1386 and KatA proteins interact. (A) Immunoprecipitation of KatA from cross-linked Δ*perR* protein lysate using an anti-KatA antibody. (B) Immunoprecipitation of Cj1386 from cross-linked Δ*perR* protein lysate using an anti-Cj1386 antibody. (A and B) Immunoprecipitated protein samples were separated by SDS-PAGE followed by immunoblotting with either anti-KatA or anti-Cj1386 antibodies to visualize protein interactions. Immunoprecipitation using an anti-Fur antibody was performed as a negative control. Purified Cj1386 and KatA proteins were run as positive controls. IP, immunoprecipitation; WB, Western blot; Input, whole-cell lysate from the Δ*perR* mutant.

using an anti-Fur antibody was performed using the Δ*perR* mutant cross-linked lysate as a negative control. Importantly, Cj1386 and KatA were not detectable when the pulldown was performed using the anti-Fur antibody. We next performed the reciprocal experiment where Cj1386 was coimmunoprecipitated from cross-linked Δ*perR* mutant lysate using an anti-Cj1386 antibody. KatA protein was detected in the Cj1386 pulldown when probed with an anti-KatA antibody (Fig. 6). Furthermore, Cj1386 and KatA were not detected in the anti-Fur-immunoprecipitated sample (Fig. 6). Overall, these results demonstrate an interaction between the KatA and Cj1386 proteins.

DISCUSSION

Catalase enzymes are one of the major H_2O_2 detoxification enzymes found within almost all respiring organisms (3). There are three distinct evolutionary classes of catalases, which include monofunctional hemin-containing catalases (including large and small subunit enzymes), bifunctional hemin-containing catalase-peroxidases, and nonhemin manganese-containing catalases (3). *C. jejuni* has only one catalase enzyme gene, *katA*, which belongs to the small-subunit, hemin-containing monofunctional class of catalases (23). Although the structure of KatA from *C. jejuni* has not been solved to date, several other catalase proteins with structural similarity to *C. jejuni* KatA have been crystalized and their structures resolved. Included among these crystal structures are KatA from *Helicobacter pylori* (56% identity) (24) and *Enterococcus faecalis* (55% identity) (21). Thus, based upon structural similarity and bioinformatic analysis, the KatA enzyme from *C. jejuni* is thought to be a tetrameric protein consisting of four identical subunits. Each subunit contains a hemin prosthetic group which is essential for facilitating the dismutation of H_2O_2 into O_2 and H_2O. The *C. jejuni* KatA protein sequence contains the conserved distal hemin ligand motif (RERIPERVVHAKG) and the proximal hemin ligand motif (RLFSYGD) (23, 25). The distal histidine residue and the proximal tyrosine residue are important for the catalytic function and coordination of hemin in catalase, respectively (25). Furthermore, expression of *katA* within *C. jejuni* is regulated primarily by Fur (15) and PerR (26). However, more recently, additional transcriptional regulators of *katA* expression have been identified, including Cj1000 (27) and CosR (28), which add additional layers of complexity to *katA* regulation. In this report, we further contribute to the wealth of knowledge on *C. jejuni* KatA by providing important insight into a key protein required for trafficking hemin to KatA.

This work identifies Cj1386 as a protein that binds hemin and trafficks it to catalase; thus, it contributes to a greater understanding of the fundamental biological processes involved in hemin trafficking within the cytoplasm and catalase biogenesis. The Cj1386 protein was found to coordinate hemin at a 1:1 heme-to-Cj1386 ratio, as determined by hemin titration assays. Bioinformatic analysis of Cj1386 reveals that it is a 17-kDa protein which contains three ankyrin repeats (23). Each ankyrin repeat consists of a series of 33 amino acids that are thought to play a role in protein-protein interactions (29). Currently, there is no structural homology model available for the Cj1386 protein. However, Cj1386 appears to represent a unique type of hemin protein, as it does not contain any previously characterized hemin-binding motif. Canonical heme/hemin motifs include those characterized for catalase as well as cytochrome proteins. Catalase coordinates hemin at the ferric ion via a tyrosine residue contained in the proximal hemin-binding motif RLFSYGD (21). Cytochrome *c* proteins typically contain a CXXCH heme-binding motif where the heme prosthetic group is covalently attached to the cytochrome at the cysteine residues (20). The heme trafficking protein CcmE from *E. coli*, which trafficks heme to periplasmic cytochrome enzymes, is covalently linked to heme at His130 (30). Heme is coordinated to the PhuS protein at the conserved His209 residue or the nonconserved His212 residue (31). Therefore, given the absence of a crystal structure or a clear hemin-binding motif, the conserved tyrosine (Y57), cysteine (C89), and histidine (H46) residues in Cj1386 were mutated to identify residues important for hemin ligand binding in Cj1386. Mutagenesis experiments revealed that Y57 is important for coordinating hemin as the Cj1386^{Y57A} protein purified in its apo form. Expression of Cj1386^{Y57A} in the *C. jejuni* Δ*cj1386*+*cj1386*^{Y57A} strain displayed a hypersensitive phenotype to H_2O_2 at levels similar to that of the Δ*cj1386* strain. Additionally, the hemin-KatA ratio in the Δ*cj1386*+*cj1386*^{Y57A} strain was significantly reduced relative to that of the wild-type strain. These results suggest that without the efficient hemin coordination seen in Cj1386^{WT}, the Cj1386^{Y57A} protein is unable to transfer hemin to KatA. Thus, KatA is unable to catalyze the dismutation of H_2O_2 into H_2O and O_2, resulting in the observed increased H_2O_2 sensitivity in the Δ*cj1386*+*cj1386*^{Y57A} strain. Mutation of the conserved histidine (H46A) or the conserved cysteine (C89A) residues did not prevent hemin binding to the Cj1386 protein during purification, and the *C. jejuni* Δ*cj1386*+*cj1386*^{H46A} or Δ*cj1386*+*cj1386*^{C89A} strain did not display an increased sensitivity to H_2O_2, indicating that H46 and C89 are not essential for hemin binding and trafficking to KatA. In the absence of Y57, the Cj1386 protein still can coordinate hemin *in vitro*. The presence of the Soret peak at 412 nm for the Cj1386^{Y57A} mutant suggests that hemin still is bound in a hexacoordinate configuration. It is possible that additional amino acids compensate for hemin binding in the absence of Y57 to produce the 6-coordinate peak. Indeed, heme coordination to PhuS in *P. aeruginosa* still can be achieved in a His209 mutant by compensation by an alternative heme coordinating residue, His212 (31). From the multiple-sequence alignment of Cj1386, a less conserved tyrosine residue (Y61), which is in close proximity to Y57, could play a role as an alternative hemin-coordinating residue. However, the UV-vis spectra also revealed the presence of an additional Soret peak at 372 nm for Cj1386^{Y57A}, suggesting pentacoordinate hemin binding. It is possible that the reduced hemin affinity at 412 nm for Cj1386^{Y57A} is insufficient to maintain the hemin in a hexacoordinate configuration, which results in a mixed population with an equilibrium of penta- and hexacoordinate binding. It is also important to note that although Y57 has been identified as being important for hemin binding, the identity of the second residue involved in the hexacoordinate binding to Cj1386 has not been identified. Importantly, we found that Cj1386 has a weaker affinity toward hemin than other characterized heme proteins, such as BSA and myoglobin. A weaker affinity toward hemin would help facilitate hemin transfer from Cj1386 to a protein with greater hemin affinity, such as KatA. Future structural studies will be required to determine the residues interacting directly with the ferric ion of hemin as well as the structure of the hemin-binding pocket.

In addition to identifying Cj1386 as a heme protein, Cj1386 also was found to transiently interact with KatA. Formaldehyde cross-linking of bacterial cultures was required to be able to detect

an interaction between Cj1386 and KatA, suggesting that after transfer of hemin, Cj1386 no longer remains associated with KatA. This finding provides strong evidence that the Cj1386 protein is trafficking hemin to KatA. Furthermore, to our knowledge, this is the first report identifying a protein which directly interacts with KatA and is important for catalase biogenesis. Cj1386 homologs are found in the *C. jejuni* strains doylei, 81-176, 81116, and S3, as well as the *Campylobacter* strains *C. coli*, *C. fetus*, *C. lari*, and *C. showae*. Interestingly, catalase-negative strains of *Campylobacter* (*C. concisus*, *C. mucosalis*, *C. sputorum*, *C. helveticus*, *C. curvus*, *C. rectus*, *C. upsaliensis*, and *C. hominis* [32, 33]) lack a homolog of Cj1386. The absence of a Cj1386 homolog in these strains suggests that Cj1386 is required only specifically for catalase biogenesis and does not play a role in trafficking hemin to other heme proteins within the cell. However, coimmunoprecipitation experiments of Cj1386 followed by mass spectrometry analysis would be required to determine any additional protein interaction partners. Cj1386 homologs also are present in other bacterial genera, including *Helicobacter*, *Arcobacter*, *Pseudomonas*, *Sulfurospirillum*, and *Acetobacter*. Cj1386 homologs are absent from bacterial species such as *E. coli*, *Salmonella*, and *Enterococcus*, suggesting that hemin trafficking to catalase occurs by other proteins or mechanisms specific to those bacterial species that have yet to be identified.

Heme uptake and transport across the periplasmic space into the cytoplasm has been well characterized for numerous bacterial species. *C. jejuni* utilizes a direct heme uptake system (ChuABCD) to acquire heme from the surrounding environment (34). This strategy for obtaining heme is analogous to the previously characterized Shu, Chu, and Phu heme acquisition systems of *Shigella dysenteriae*, *E. coli*, and *P. aeruginosa* (35–37). The *C. jejuni* heme uptake system encodes the outer membrane heme receptor (ChuA), which transports heme across the outer bacterial membrane in a TonB-ExbB-ExbD energy-dependent manner (23, 34). Heme then is transported across the periplasmic space by the periplasmic transport protein ChuD and finally across the inner membrane by the ABC transport complex, ChuBC (34). The proteins and mechanism for which Cj1386 obtains hemin within the cytoplasm currently are uncharacterized; however, the ChuBC complex may play a role in this process.

In summary, we have identified Cj1386 as a hemin-binding protein which displays a weaker affinity toward hemin than other heme proteins. This characteristic likely is essential for facilitating hemin transfer to KatA. Additionally, we have identified tyrosine 57 as a critical residue required for optimal Cj1386 function within *C. jejuni*. Future structural studies of Cj1386 should provide key insights into the hemin coordination sites and hemin-binding pocket of this unique hemin-trafficking protein.

ACKNOWLEDGMENTS

This work was supported by CIHR funding (MOP 84224) to A.S. and a QEIIGSST scholarship to A.F.

REFERENCES

1. **Imlay JA.** 2003. Pathways of oxidative damage. Annu Rev Microbiol **57:** 395–418. http://dx.doi.org/10.1146/annurev.micro.57.030502.090938.
2. **Imlay JA.** 2008. Cellular defenses against superoxide and hydrogen peroxide. Annu Rev Biochem **77:**755–776. http://dx.doi.org/10.1146/annurev.biochem.77.061606.161055.
3. **Zamocky M, Gasselhuber B, Furtmuller PG, Obinger C.** 2012. Molecular evolution of hydrogen peroxide degrading enzymes. Arch Biochem Biophys the **525:**131–144. http://dx.doi.org/10.1016/j.abb.2012.01.017.
4. **Zamocky M, Furtmuller PG, Obinger C.** 2008. Evolution of catalases from bacteria to humans. Antioxid Redox Signal **10:**1527–1548. http://dx.doi.org/10.1089/ars.2008.2046.
5. **Chelikani P, Fita I, Loewen PC.** 2004. Diversity of structures and properties among catalases. Cell Mol Life Sci **61:**192–208. http://dx.doi.org/10.1007/s00018-003-3206-5.
6. **Baureder M, Hederstedt L.** 2012. Genes important for catalase activity in Enterococcus faecalis. PLoS One **7:**e36725. http://dx.doi.org/10.1371/journal.pone.0036725.
7. **Flint A, Sun YQ, Stintzi A.** 2012. Cj1386 is an ankyrin-containing protein involved in heme trafficking to catalase in Campylobacter jejuni. J Bacteriol **194:**334–345. http://dx.doi.org/10.1128/JB.05740-11.
8. **Sheffield P, Garrard S, Derewenda Z.** 1999. Overcoming expression and purification problems of RhoGDI using a family of "parallel" expression vectors. Protein Expr Purif **15:**34–39. http://dx.doi.org/10.1006/prep.1998.1003.
9. **Ascoli F, Fanelli MR, Antonini E.** 1981. Preparation and properties of apohemoglobin and reconstituted hemoglobins. Methods Enzymol **76:** 72–87. http://dx.doi.org/10.1016/0076-6879(81)76115-9.
10. **Kobayashi C, Suga Y, Yamamoto K, Yomo T, Ogasahara K, Yutani K, Urabe I.** 1997. Thermal conversion from low- to high-activity forms of catalase I from Bacillus stearothermophilus. J Biol Chem **272:**23011–23016. http://dx.doi.org/10.1074/jbc.272.37.23011.
11. **Altschul SF, Madden TL, Schaffer AA, Zhang J, Zhang Z, Miller W, Lipman DJ.** 1997. Gapped BLAST and PSI-BLAST: a new generation of protein database search programs. Nucleic Acids Res **25:**3389–3402. http://dx.doi.org/10.1093/nar/25.17.3389.
12. **Sievers F, Wilm A, Dineen D, Gibson TJ, Karplus K, Li W, Lopez R, McWilliam H, Remmert M, Soding J, Thompson JD, Higgins DG.** 2011. Fast, scalable generation of high-quality protein multiple sequence alignments using Clustal Omega. Mol Syst Biol **7:**539. http://dx.doi.org/10.1038/msb.2011.75.
13. **Goujon M, McWilliam H, Li W, Valentin F, Squizzato S, Paern J, Lopez R.** 2010. A new bioinformatics analysis tools framework at EMBL-EBI. Nucleic Acids Res **38:**W695–W699. http://dx.doi.org/10.1093/nar/gkq313.
14. **Waterhouse AM, Procter JB, Martin DM, Clamp M, Barton GJ.** 2009. Jalview version 2–a multiple sequence alignment editor and analysis workbench. Bioinformatics **25:**1189–1191. http://dx.doi.org/10.1093/bioinformatics/btp033.
15. **Butcher J, Sarvan S, Brunzelle JS, Couture JF, Stintzi A.** 2012. Structure and regulon of Campylobacter jejuni ferric uptake regulator Fur define apo-Fur regulation. Proc Natl Acad Sci U S A **109:**10047–10052. http://dx.doi.org/10.1073/pnas.1118321109.
16. **Lykkegaard MK, Ehlerding A, Hvelplund P, Kadhane U, Kirketerp MB, Nielsen SB, Panja S, Wyer JA, Zettergren H.** 2008. A Soret marker band for four-coordinate ferric heme proteins from absorption spectra of isolated Fe(III)-Heme+ and Fe(III)-Heme+(His) ions in vacuo. J Am Chem Soc **130:**11856–11857. http://dx.doi.org/10.1021/ja803460c.
17. **Rao F, Ji Q, Soehano I, Liang ZX.** 2011. Unusual heme-binding PAS domain from YybT family proteins. J Bacteriol **193:**1543–1551. http://dx.doi.org/10.1128/JB.01364-10.
18. **Smulevich G, Neri F, Marzocchi MP, Welinder KG.** 1996. Versatility of heme coordination demonstrated in a fungal peroxidase. Absorption and resonance Raman studies of Coprinus cinereus peroxidase and the Asp245–>Asn mutant at various pH values. Biochemistry **35:**10576–10585.
19. **Bhakta MN, Wilks A.** 2006. The mechanism of heme transfer from the cytoplasmic heme binding protein PhuS to the delta-regioselective heme oxygenase of Pseudomonas aeruginosa. Biochemistry **45:**11642–11649. http://dx.doi.org/10.1021/bi060980l.
20. **Travaglini-Allocatelli C.** 2013. Protein machineries involved in the attachment of heme to cytochrome c: protein structures and molecular mechanisms. Scientifica **2013:**505714. http://dx.doi.org/10.1155/2013/505714.
21. **Hakansson KO, Brugna M, Tasse L.** 2004. The three-dimensional structure of catalase from Enterococcus faecalis. Acta Crystallogr D Biol Crystallogr **60:**1374–1380. http://dx.doi.org/10.1107/S0907444904012004.
22. **Pellicer S, Gonzalez A, Peleato ML, Martinez JI, Fillat MF, Bes MT.** 2012. Site-directed mutagenesis and spectral studies suggest a putative role of FurA from Anabaena sp. PCC 7120 as a heme sensor protein. FEBS J **279:**2231–2246. http://dx.doi.org/10.1111/j.1742-4658.2012.08606.x.
23. **Parkhill J, Wren BW, Mungall K, Ketley JM, Churcher C, Basham D,**

Chillingworth T, Davies RM, Feltwell T, Holroyd S, Jagels K, Karlyshev AV, Moule S, Pallen MJ, Penn CW, Quail MA, Rajandream M-A, Rutherford KM, Vliet AHMV, Whitehead S, Barell BG. 2000. The genome sequence of the food-borne pathogen *Campylobacter jejuni* reveals hypervariable sequences. Nature **403:**665–668. http://dx.doi.org/10.1038/35001088.

24. **Loewen PC, Carpena X, Rovira C, Ivancich A, Perez-Luque R, Haas R, Odenbreit S, Nicholls P, Fita I.** 2004. Structure of Helicobacter pylori catalase, with and without formic acid bound, at 1.6 A resolution. Biochemistry **43:**3089–3103. http://dx.doi.org/10.1021/bi035663i.
25. **Alyamani EJ, Brandt P, Pena JA, Major AM, Fox JG, Suerbaum S, Versalovic J.** 2007. Helicobacter hepaticus catalase shares surface-predicted epitopes with mammalian catalases. Microbiology **153:**1006–1016. http://dx.doi.org/10.1099/mic.0.29184-0.
26. **van Vliet AH, Baillon ML, Penn CW, Ketley JM.** 1999. Campylobacter jejuni contains two fur homologs: characterization of iron-responsive regulation of peroxide stress defense genes by the PerR repressor. J Bacteriol **181:**6371–6376.
27. **Dufour V, Li J, Flint A, Rosenfeld E, Rivoal K, Georgeault S, Alazzam B, Ermel G, Stintzi A, Bonnaure-Mallet M, Baysse C.** 2013. Inactivation of the LysR regulator Cj1000 of Campylobacter jejuni affects host colonization and respiration. Microbiology **159:**1165–1178. http://dx.doi.org/10.1099/mic.0.062992-0.
28. **Hwang S, Zhang Q, Ryu S, Jeon B.** 2012. Transcriptional regulation of the CmeABC multidrug efflux pump and the KatA catalase by CosR in Campylobacter jejuni. J Bacteriol **194:**6883–6891. http://dx.doi.org/10.1128/JB.01636-12.
29. **Bennett V.** 1992. Ankyrins. Adaptors between diverse plasma membrane proteins and the cytoplasm. J Biol Chem **267:**8703–8706.
30. **Harvat EM, Redfield C, Stevens JM, Ferguson SJ.** 2009. Probing the heme-binding site of the cytochrome c maturation protein CcmE. Biochemistry **48:**1820–1828. http://dx.doi.org/10.1021/bi801609a.
31. **Block DR, Lukat-Rodgers GS, Rodgers KR, Wilks A, Bhakta MN, Lansky IB.** 2007. Identification of two heme-binding sites in the cytoplasmic heme-trafficking protein PhuS from Pseudomonas aeruginosa and their relevance to function. Biochemistry **46:**14391–14402. http://dx.doi.org/10.1021/bi701509n.
32. **Bourke B, Chan VL, Sherman P.** 1998. Campylobacter upsaliensis: waiting in the wings. Clin Microbiol Rev **11:**440–449.
33. **Lawson AJ, On SL, Logan JM, Stanley J.** 2001. Campylobacter hominis sp. nov., from the human gastrointestinal tract. Int J Syst Evol Microbiol **51:**651–660. http://dx.doi.org/10.1099/00207713-51-2-651.
34. **Ridley KA, Rock JD, Li Y, Ketley JM.** 2006. Heme utilization in Campylobacter jejuni. J Bacteriol **188:**7862–7875. http://dx.doi.org/10.1128/JB.00994-06.
35. **Wyckoff EE, Duncan D, Torres AG, Mills M, Maase K, Payne SM.** 1998. Structure of the Shigella dysenteriae haem transport locus and its phylogenetic distribution in enteric bacteria. Mol Microbiol **28:**1139–1152. http://dx.doi.org/10.1046/j.1365-2958.1998.00873.x.
36. **Ochsner UA, Johnson Z, Vasil ML.** 2000. Genetics and regulation of two distinct haem-uptake systems, phu and has, in Pseudomonas aeruginosa. Microbiology **146**(Part 1)**:**185–198.
37. **Tong Y, Guo M.** 2009. Bacterial heme-transport proteins and their heme-coordination modes. Arch Biochem Biophys **481:**1–15. http://dx.doi.org/10.1016/j.abb.2008.10.013.
38. **Palyada K, Sun YQ, Flint A, Butcher J, Naikare H, Stintzi A.** 2009. Characterization of the oxidative stress stimulon and PerR regulon of Campylobacter jejuni. BMC Genomics **10:**481. http://dx.doi.org/10.1186/1471-2164-10-481.
39. **Yao R, Alm RA, Trust TJ, Guerry P.** 1993. Construction of new Campylobacter cloning vectors and a new mutational cat cassette. Gene **130:**127–130. http://dx.doi.org/10.1016/0378-1119(93)90355-7.
40. **Reid AN, Pandey R, Palyada K, Naikare H, Stintzi A.** 2008. Identification of Campylobacter jejuni genes involved in the response to acidic pH and stomach transit. Appl Environ Microbiol **74:**1583–1597. http://dx.doi.org/10.1128/AEM.01507-07.
41. **Gattoni M, Boffi A, Sarti P, Chiancone E.** 1996. Stability of the heme-globin linkage in alphabeta dimers and isolated chains of human hemoglobin. A study of the heme transfer reaction from the immobilized proteins to albumin. J Biol Chem **271:**10130–10136.
42. **Hargrove MS, Barrick D, Olson JS.** 1996. The association rate constant for heme binding to globin is independent of protein structure. Biochemistry **35:**11293–11299. http://dx.doi.org/10.1021/bi960371l.